

COMPLIANT FINGERS MAKE SIMPLE SENSORS SMART

Leif P. Jentoft

School of Engineering and Applied Sciences
Harvard University
Email: ljentoft@seas.harvard.edu

Robert D. Howe

School of Engineering and Applied Sciences
Harvard University
Email: howe@seas.harvard.edu

ABSTRACT

Compliance in robot hands has been shown to enhance grasping performance and robustness. This paper presents analysis and experiments to show that compliance also enables measurement of important object parameters using simple joint angle sensors. Compliance reduces control requirements so that it is easy to trace object surfaces, while joint angle measurements can reveal contact locations and contact force vectors. While these techniques are limited in the complexity of the contact situations where they can be applied, they are highly effective in many situations, and can be implemented at very low cost due to their use of existing joint angle sensors.

1 INTRODUCTION

Hand compliance helps robotic grasping by providing adaptability and robustness. In unstructured environments, uncertainties are large, and target object size and location may be poorly known. Finger compliance allows the gripper to conform to objects while minimizing contact forces.

Low joint stiffness can also enhance the robustness of robot grippers: unintended contact can result in large contact forces unless the gripper is compliant. In previous work we have demonstrated that compliance can enable effective grasping despite object uncertainties [1], but sensing must fill a crucial role in real-world applications. Sensing of object properties will improve grasping performance [2], and is essential in situations where other sources of information are inadequate, such as visual occlusion.

A vast number of tactile sensors have been developed for robotics research. These range from simple binary sensors that detect contact to elaborate tactile array sensors that can estimate contact location, object curvature and contact pressure distribution [3-7]. Few tactile sensors have been integrated with robot hands and used for control of grasping or manipulation. The

usual approach that has been posited is to use the sensor information in active hand control, i.e. position or force control of the fingers. This places severe demands on control precision, as changes in finger position with respect to the object can result in large changes in contact force with traditional stiff position-controlled finger designs. Such transients will corrupt tactile sensor readings, in turn making it difficult to use contact information for control or perception.

One way to avoid the issues of complexity and fragility with conventional tactile sensors is to replace fully-actuated stiff fingers with compliant underactuated fingers. This allows considerable information to be obtained from simple sensors. One benefit is the relaxation of control precision requirements: mechanical compliance maintains stable contact forces despite imprecise hand position with respect to the object. This simplifies sliding of the fingers over object surfaces, for example to determine shape during the grasping process. The presence of multiple compliant joints within the finger enables estimation of contact location from joint angle measurements, by using kinematics and torque equilibrium constraints. A similar approach can yield contact and force estimates.

In this paper we explore the use of simple joint angle sensors with compliant fingers to derive a variety of information about target objects. We begin with a brief review of the mechanics of our compliant hand, followed by a description of the design of a low-cost joint angle sensor for flexure joints. We then present three examples of methods for using these sensors to determine object properties. The first is estimating object shape through tracing, where compliance reduces control constraints. Next, we show that changing hand posture allows sensing of contact location. Finally, we use contact location estimates and joint positions to find contact forces. The concluding section examines the benefits and limitations of this approach.

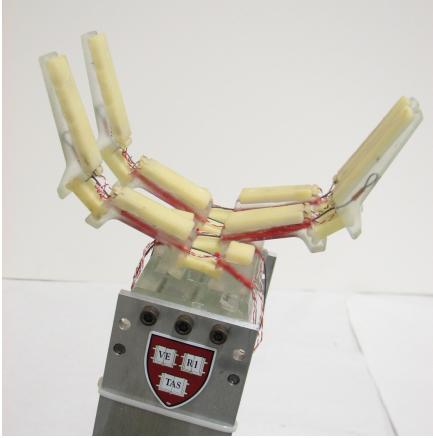


Figure 1. SDM HAND AND ACTUATION SCHEMATIC

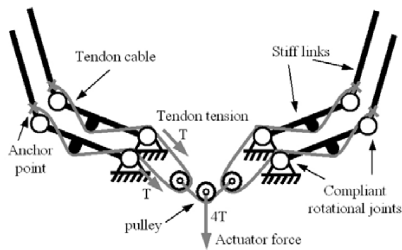


Figure 2. ACTUATION SCHEMATIC OF THE SDM HAND

2 Finger and Sensor Design

The sensing strategy described here is based on the premise that the fingers are highly compliant, i.e. low contact forces are generated as the joints deflect over a significant angular range. In addition to enabling new sensing strategies, this provides good grasping capabilities in unstructured environments and mechanical robustness. Our finger design is based on the use of flexures, which simplifies fabrication and reduces costs, but makes joint angle sensing more difficult.

2.1 SDM Hand

Before describing the sensing work that is the focus of this paper, we provide a brief overview of the design and function of the SDM Hand (Fig.1). An extensive description can be found in [8]. As the name suggests, the hand was fabricated using polymer-based Shape Deposition Manufacturing (SDM) [9, 10] to provide compliance and robustness. SDM is a layered manufacturing technique with which the rigid links and compliant joints of the gripper are created simultaneously with embedded sensing and actuation components. Elastomeric flexures create compliant joints, eliminating metal bearings, and tough rigid

polymers fully encase the embedded components, eliminating the need for seams and fasteners that are often the source of mechanical failure.

The preshape, stiffness, and joint coupling characteristics of the hand were determined based on the results of previously conducted optimization studies [11, 12]. In these simulations, the joint rest angles, joint stiffness ratio, and coupling scheme of the hand were varied and the performance analyzed to maximize the allowable uncertainty in object location and size as well as minimize contact forces.

The concave side of each finger link contains a soft fingerpad to maximize friction and contact area, thereby increasing grasp stability. Links are connected via elastomer joint flexures, designed to be compliant in the plane of finger motion and stiffer out of plane. Due to the molding process used to create them, the SDM fingers, with embedded sensors and actuation components, are a single lightweight part (39 grams each), with no fasteners or adhesives.

The polyurethane used for the joints of the fingers demonstrates significant viscoelastic behavior, providing both compliance and passive damping to the hand. The damping in the joints is necessary to reduce joint oscillations and permit the use of low joint stiffness. The joints can also undergo large deflections while remaining completely functional. The advantages of this property are clear when considering the damage that can result due to large contact forces that can occur with unplanned contact during use of traditional stiff robotic hands.

For actuation, each finger has a pre-stretched, nylon-coated stainless steel cable anchored into the distal link, and running through low-friction tubing to the base. The transmission of the hand is arranged such that the compliance in the fingers is in parallel with the actuator. Before the hand is actuated, the tendon cable remains slack and the finger is in its most compliant state. This method permits the use of actuators that are not backdrivable and prevents the inertial load of the actuator from increasing the passive stiffness. After actuation, the stiff tendon takes much of the compliance out of the fingers, resulting in a stiffer grasp with greater stability. This arrangement of the compliance in parallel with the actuation is a key factor in the effective performance of the hand.

A single actuator drives the four fingers (eight joints) of the hand. This not only makes the gripper simpler and lighter, but it also allows the gripper to be self-adapting to the target object. Fig 2 details the actuation scheme, by which motion of the distal links can continue after contact on the coupled proximal links occurs, allowing the finger to passively adapt to the object shape. Additionally, the pulley design in this scheme allows the remaining fingers to continue to enclose the object after the other fingers have been immobilized by contact, ensuring that an equal amount of tension is exerted on each tendon cable, regardless of finger position or contact state.

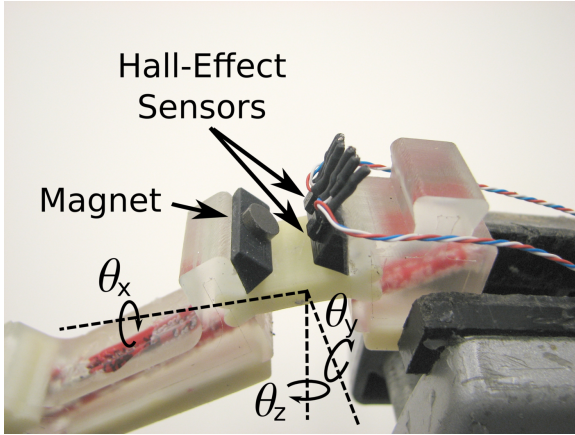


Figure 3. JOINT-ANGLE SENSORS ON BASE FINGER JOINT

2.2 Sensors

Joint angle sensors are probably the most ubiquitous sensors for robotics, due to their importance for basic manipulator control. This makes them attractive for object sensing applications as well. Traditional joint-angle sensors such as encoders that rely on a single axis of motion, however, are poorly suited to flexure joints due to the complicated relative motion of the adjacent links. Vision-based systems that use markers to track the position and orientation of a link are potentially useful, but they require a direct line-of-sight to the fingers, which may be difficult to achieve. This is especially true when exploring constrained spaces (such as handles and holes) where tactile sensors are often most useful to determine grasping affordances.

Other alternatives for measuring bending angles of flexures include materials that change resistance with deflection (e.g. piezoresistive rubber), but these often suffer from hysteresis. Fiber optic flexion sensors are potentially useful but are relatively expensive. In light of these issues, hall-effect sensors were chosen for their low hysteresis, low drift, minimal cost, and the ease with which they can be molded inside fingers using the SDM process. For this initial proof-of-concept, the prototype sensors are mounted on the outside of the fingers, though in a final system they would be molded into the fingers directly.

The Hall effect is based on the deflection of a current in a magnetic field due to Lorentz force acting on the electrons passing through the sensor [13]. Thus, the response of the Hall-effect sensor near a magnet is dependant on both the orientation and the distance of the sensor from the magnet. The power of the magnetic field falls off as $1/r^3$ with respect to distance, and the direction of the field changes depending on the magnetic latitude. Moving from pole to the equator, the magnetic field transitions from parallel to perpendicular to antiparallel to the axis of the magnet.

To keep the sensor response monotonic under large deflec-

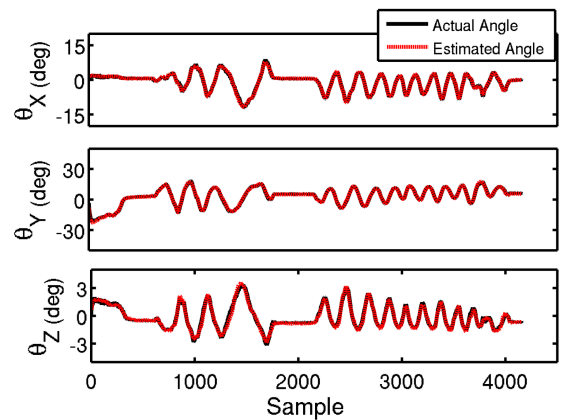
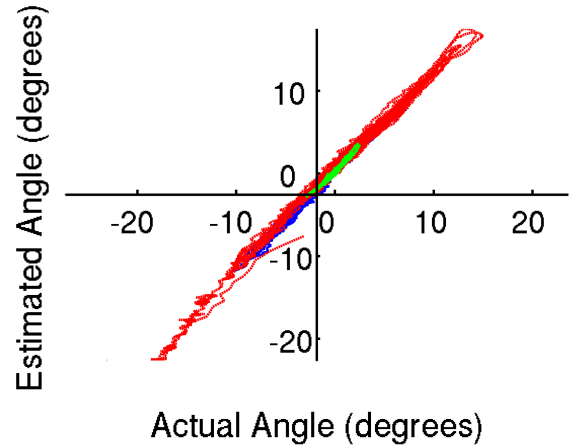


Figure 4. JOINT-ANGLE SENSOR CALIBRATION: RESPONSE PLOT (ABOVE) AND CALIBRATION SAMPLE (BELOW)

tions of the elastic joint, the sensors (A1321EUA 5mV/G, Allegro Microsystems Inc) were mounted at an angle of 60 degrees relative to the magnet as shown in Fig. 3 to synchronize the effects of changing the distance to the magnet and changing the orientation of the magnet. A mounting site on the outside of the finger was chosen to minimize magnetic interference from grasping ferrous objects and to maximize the sensitivity of the sensors as the fingers are pushed apart.

To relate the readings from the hall-effect sensors to the deflection of the joints, we used an experimentally-based calibration that includes the effect of the joint transmission and variations in the precise locations of the magnets (important when casting such parts in SDM). For this step, the finger link attached to the joint of interest was fitted with a electromagnetic tracking device (Flock of Birds MiniBird, Ascension Technologies, Inc.) to measure the actual orientation of the finger. Voltage readings from the hall-effect sensors (A1321EUA 5mV/G, Allegro Microsystems Inc) were captured at 1Khz with 16bit precision by

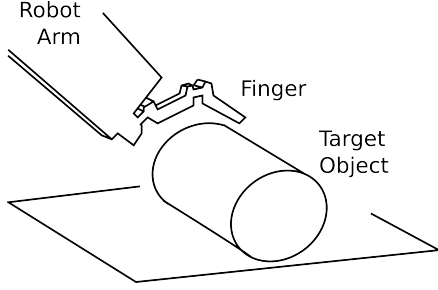


Figure 5. EXPERIMENTAL SETUP: FINGER MOUNTED ON WAM ARM IS DRAGGED ACROSS A CYLINDRICAL TARGET.

the embedded system that controls the arm (DS1103., dSpace Inc). A string was attached to the tip of the finger, and a sharp deflection was applied to allow the synchronization of the two readings. The finger tip was then perturbed in all three axes over the course of several seconds.

A reduced-term Taylor approximation of the joint angles in terms of the sensor voltages was computed as follows:

$$\theta_1(V_0, V_1) = a_1V_0 + a_2V_0^2 + a_3V_0^3 + a_4V_1 + a_5V_1^2 + a_6V_1^3 + a_7V_1V_2 \quad (1)$$

Note this is a third-order taylor expansion with some of the higher-order cross-terms removed. Put in matrix form, this is

$$\vec{\theta} = \mathbf{A}[V_0, V_0^2, V_0^3, V_1, V_1^2, V_1^3, V_1V_2]^T \quad (2)$$

The voltages from the trial were preprocessed (offset by the resting voltage, and then squared, cubed, multiplied) and put in vector form above, and the matrix equation was solved for a least-squares fit using singular value decomposition (SVD) to yield the calibration matrix \mathbf{A} . These results generated a fit for the x-angle (twist), y-angle (extension/flexion), and z-angle (abduction/adduction). Across a range of 20°, 40°, and 7°, respectively, this resulted in an average accuracy of 0.29°, 0.45°, and 0.13° across the trial, with maximum errors 1.75°, 4.2°, and 0.8° (see Fig.4).

3 Object Tracing

3.1 Concept

One key aspect of characterizing an object is determining its surface boundaries. Given a known contact location on the finger, it is possible to draw the finger across the object and calculate the object boundaries using a simple forward-kinematics model. To do so with the SDM Hand, we set up a kinematic chain composed of four kinematic frames; the world frame, the hand frame, the

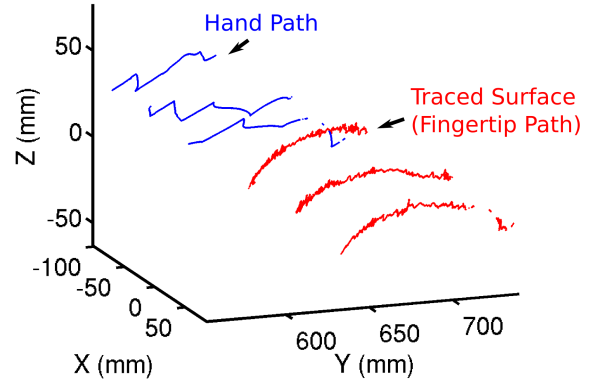


Figure 6. TRACING RESULTS: THREE PASSES ALONG THE TARGET OBJECT. NOTE JAGGED HAND TRAJECTORY AND SMOOTH SURFACE TRACKING.

link1 frame, and the link2 frame as shown in Fig. 7; each of these is fully defined by a translation and an orientation (rotation) relative to the last coordinate frame.

Then, a contact point on the second link can be depicted as

$$\vec{c}_w = \mathbf{R}_{hand}(\mathbf{R}_1(\mathbf{R}_2\vec{c}_2 + \vec{T}_1) + \vec{T}_{hand} \quad (3)$$

where \vec{c}_w is the location of the contact in the world frame, \vec{c}_2 is the location of the contact in the link2 frame, \mathbf{R}_2 is the rotation matrix that defines the rotation from joint 2 to joint 1, \vec{T}_2 defines the related translation, and \mathbf{R}_{hand} , \mathbf{R}_1 and \vec{T}_1 and \vec{T}_{hand} are similarly defined.

3.2 Algorithm

To determine whether there is an object at the tip of the finger, two questions must be answered—is the finger deflected due to an object, and if so, is the object at the tip.

Contact with an object can be detected by the deflection of the finger from the expected position. In this experiment, we use a simple static model for the expected position of the fingers. A more sophisticated dynamic model would allow the elimination of deflections due to purely inertial effects as well as the elimination of the path as the finger swings back from contact based on the expected return velocity of the finger.

Thus, the more important assumption made here is that the deflection occurs from a single contact on the tip of the finger. There are several ways to test whether this is a tenable assumption, including minimum-energy analysis of the joint deflections, comparing multiple readings as in sec. 4, or using a single tactile sensor at the tip of the finger.

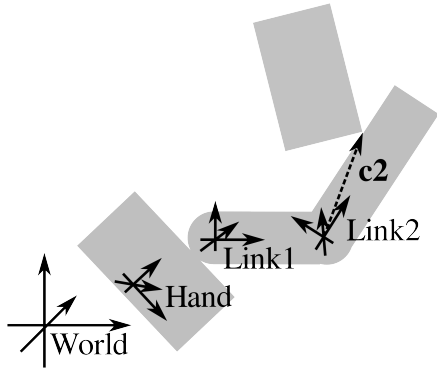


Figure 7. LINK COORDINATE FRAMES: WORLD, HAND, LINK1, AND LINK2

3.3 Validation

This approach was experimentally validated with a trial shown in Fig. 5. A cylindrical object (diameter 127 mm) was mounted on a fixed table and a finger was brushed against it several times. The deflection of the finger was sampled at 1Khz and noise was removed with a 10-sample running average. The deflection angle was then thresholded at 7.5, 7.2, and 2.6 degrees for the x, y, and z angles to give the regions where the finger was in contact with the object. Results are shown in Fig 6.

Due to the difference in the stiffness between the proximal and the distal finger joints, the deflection of the base joint dominates the finger motion when forces are not directly down the axis of the tip of the finger. In light of this, the system at the time of the experiment only read angles from two joint-angle sensors on the base joint although future plans will also include the distal joint. Note that the deflection around the x-axis (which points in the direction of the fingertip) and the deflection around the z-axis (normal to the pad) are thus coupled when the finger is pushed from the fingertip, which enables three angles of deflection to be measured with two sensors.

4 Contact Localization

4.1 Concept

The location on the finger of the contact with an object is a key factor in the mechanical interaction of the hand-object system. Contact location can be directly measured using tactile array sensors, but these devices are complex, expensive, and challenging to integrate with the finger structure [7]. An appealing alternative is to measure the deflection of an elastic structure with a sensor at the base, a robotic analog of biological systems such as whiskers and antennae. The methodology to determine contact location from the deflection of a continuous elastic beam has been studied in the context of rat whiskers [16] and robotics [17], but these approaches are less useful here where compliance oc-

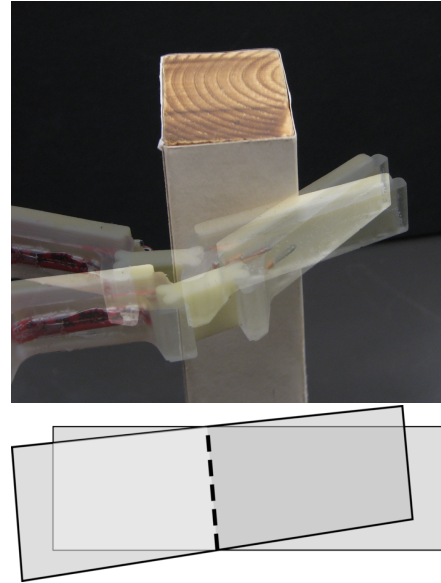


Figure 8. CONTACT LOCALIZATION FROM INTERSECTION OF FINGER GEOMETRY (PARTIAL LOCATION CONSTRAINT)

curs at discrete joints.

An alternate approach to determining contact location from joint-angle sensors has been proposed by Kaneko et. al; in [14]; this uses two readings to determine the position of a contact on a finger with planar geometry by stroking the finger along it using active compliance. The active control approach requires torque sensors and a precise control system to avoid perturbing the object during the stroke. Replacing active compliance with passive compliance allows these principles to be extended to a lower-tolerance system without torque sensors.

Here we consider a more general approach that extends this to arbitrary finger geometry. The concept is based on comparing two joint sensor readings, taken before and after a slight perturbation of the finger location due to motion of the robot hand. At each reading, the location of the contact surface of the finger is known from the forward kinematics of the system and the finger geometry. The algorithm then finds the intersection of the finger contact surfaces, which are the presumed contact locations. Because there may be several potential intersections, it is then necessary to determine which is most likely, which can be done based on the known motion of the hand and minimum-energy analysis of the elastic joints.

Since the finger in our prototype hand has two joints, we use four kinematic frames as follows, though the methodology readily extends to additional degrees of freedom. The link2 frame is expressed relative to the link1 frame, expressed relative to the hand frame, expressed in world frame coordinates. Each is fully defined by an position-vector origin \vec{P} and a rotation matrix \mathbf{R} .

Then, the location of an arbitrary contact vector \vec{c}_1 on link 1 can be expressed in world as

$$\vec{c}_w = \mathbf{R}_h(\mathbf{R}_1\vec{c}_1 + \vec{P}_1) + \vec{P}_h \quad (4)$$

Likewise for an arbitrary contact vector \vec{c}_2 on link 2

$$\vec{c}_w = \mathbf{R}_h(\mathbf{R}_1(\mathbf{R}_2\vec{c}_2 + \vec{P}_2) + \vec{P}_1) + \vec{P}_h \quad (5)$$

When the geometry of the fingertip is known, it is possible to express vector \vec{c} in terms of the known constraints of the finger. This is especially straightforward when the finger can be composed of planes, as is the case with our prototype and many other robotic fingers; in this case we model each link as a rectangular prism composed of four such faces. If each plane is expressed as a set of two vectors: a normal vector \hat{n}_i and a point in the plane, \vec{x}_i , we can project these parameters through the finger kinematics for link 1 as

$$\hat{n}'_i = \mathbf{R}_h\mathbf{R}_1\hat{n}_i \quad (6)$$

and

$$\vec{x}'_i = \mathbf{R}_h(\mathbf{R}_1\vec{x}_i + \vec{P}_1) + \vec{P}_h \quad (7)$$

The projection for link2 follows similarly with an additional rotation and translation.

Thus, the planar surface constraints can be converted to a linear equation that can be easily solved either for a direct solution, or, if multiple readings are taken to reduce the effects of noise, for a least-squares best fit. In three dimensions, it requires three linearly independent planes to fully define the point of intersection. With only two different planes, it is still possible to obtain useful information by bounding the resulting line by the limits of the fingerpad surface.

If two planes are very close to parallel, the location of their intersection is very sensitive to the angle between them. At such small configuration differences, this angle will be dominated by sensor noise, so it is beneficial to ensure sufficient difference between tested configurations. When a section of the finger does not move, it is possible to generate a degenerate state where the finger surface constraints project to the same equation in world frame. This can be avoided by selecting an appropriate probing algorithm that controls the approach direction.

This method can be applied to each pair of surfaces between configurations of the finger to determine a list of potential contacts; to reduce the computation time, it is possible to choose a subset of the surfaces based on which are most likely to contact an object given the direction of motion (e.g., skipping surfaces on the back side of the finger).

It is possible to narrow this list of possible solutions by comparing each contact location to the known extent of the link on which it occurs. It is possible to further reduce this set by assuming a single contact point and analyzing the minimum-energy configurations of the elastic joints. For example, with a single contact point, a potential contact point on the side of link2 will never cause antagonistic deflection of link1 and link2 and thus such a reading would inform the decision that an intersection on the fingertip would be the more likely contact point.

This algorithm makes only the assumption that the contact must occur on a fixed point on the object—if both the location of the contact on the finger and the location of the contact on the object move, little information can be gained beyond the fact that the contact is somewhere outside the boundary of the finger surface. Although sliding the finger along the object does not necessarily break the assumption of a fixed contact location on the object, many fingers are axially symmetric and this thus generates little change in the geometry of the finger and results in a poorly defined set of intersections.

Thus, the algorithm should approach the expected position of the surface in the same direction as the normal vector to the finger pad. When contact occurs in this situation, the finger will deflect and the position of the contact will roll along the surface of the object slightly. This will yield a conservative estimate of the contact location slightly outside the surface of the object as observed in [14]. Note that if precise characterization is required, increasing the accuracy of the joint-angle sensor can reduce this error.

4.1.1 Algorithm

1. From each pair of (possibly) intersecting surfaces from two configurations, project surface constraints to the world frame
2. Test projected constraints to ensure there is sufficient difference between them to overcome sensor noise
3. Solve for the intersection of the surface constraints
4. Test whether this intersection occurs within the extent of the finger surface
5. Test whether contact at this location is consistent with a minimum-energy deflection of the finger joints

5 Forces

Finally, note that these methods allow the computation of the forces exerted while probing an object based on the deflection of

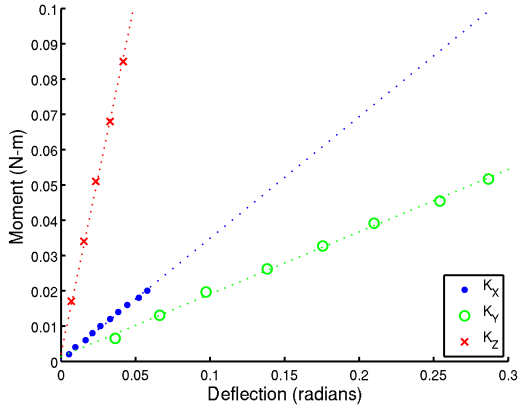


Figure 9. JOINT SPRING CONSTANTS

the elastic joints. We define the stress-strain tensor for the joint as \mathbf{K} and assume the spring behavior of the joint is linear around rest position. We can then relate the deflection of the joint to $\vec{\theta}$ to the moment exerted by it against this deflection as follows:

$$\vec{\tau} = \mathbf{K}\vec{\theta} \quad (8)$$

However, from section 4, we can also determine the location of the contact. From this, it is possible to determine the force exerted at that point via

$$\vec{F} = \vec{\tau} \times \vec{R} \quad (9)$$

For the SDM finger, the moment-strain curve along each of the primary axes was measured and is as shown in Fig. 9; measurements have been overlaid with a first-order linear fit to show the behavior near the rest position. From this, it is clear that the joint is least stiff around the y-axis and thus that contact in line with the pad will generate the least force. In the finger tracing experiment, the tip is at a radius of $\vec{r} = [7, 13, 13]$ cm from the joint, and given the maximum deflection of the joint during the experiment, the total force from the deflection of the base joint is less than 0.1N. This measurement does not include the effects of loads in line with the joint (though these can be detected by measuring the deflection of the second joint), but similar performance is anticipated with an appropriate choice of approach path that keeps the contact on the pad of the fingertip rather than directly on the end.

6 Discussion

These results illustrate useful methods for sensing interactions with the outside world using only joint angle sensors. These

intrinsic sensors are internal to the robot structure [18] and are provided in virtually all manipulators for basic control of position and force. Joint compliance allows the inference of a variety of external object and contact properties using only these sensor signals. This minimizes system complexity and fabrication costs.

Compliance helps with sensing in several different ways. For determining object shape through tracing, compliance greatly reduces control precision requirements. Only the approximate object shape is required to define a satisfactory hand trajectory, and the low finger stiffness ensures that the finger will remain in contact with only moderate variations in contact force. To do this with a stiff finger would require accurate contact force sensing and real-time trajectory adjustment to maintain satisfactory forces. Similar considerations apply to estimating contact location from joint angles, where finger compliance maintains contact for a range of hand motions.

For contact force estimation, compliance is essential to the sensing process because it is based on the causal relationship between contact force and deflection of the joint. Furthermore, forces can only be sensed in the directions that the joint moves. Thus a compliant joint constructed as a spring around a conventional pin joint with a single axis of motion can only detect the torque about that axis. For the elastomer flexures in our SDM Hand, the resolution of the force sensing algorithm in each axis will vary with compliance of the flexure in that axis. It may be possible to tune the sensitivity of the joint angle sensor to match the motion resolution to the anticipated deflection in each axis.

For simplicity, the techniques illustrated here use only sensing at a single joint. This is reasonable for our SDM hand prototype, because the distal joint is much stiffer (and thus deflects less) than the proximal joint in order to maximize grasping capture range [12]. Future work will explore the benefits of combining sensor readings from multiple joints. We anticipate that this will augment sensing accuracy and help with disambiguation of contact location type (e.g. line vs. point contacts). Preliminary analysis suggests that multiple joint reading can disambiguate multiple points of contact along different links, which will address a significant limitation of the approach (below).

A central limitation of the proposed approach is that it is based on the assumption of a single contact between the finger and object. This is reasonable for probing situations, where contact at the tip of the finger is desired and can be readily checked using multiple joint angle measurements. The methods outlined in section 4 may be used to periodically check the single-contact assumption, but when the finger is constrained by multiple points of contact, deadlock situations may arise, as noted in [14]. Some of these may be detected by comparing the state of the finger to minimum-energy configurations of the elastic finger joints, and is also possible to minimize the occurrence of this problem through appropriate motion algorithms for the approach trajectory. The use of additional sensors, e.g. simple binary contact detectors [2], can also serve to resolve multiple contact problems.

Other assumptions are related to the frictional properties of the fingers. For example, the object shape tracing scheme relies on smooth sliding, and the contact localization estimate assumes that the contact location remains fixed as the finger pivots on the contact feature. This will require good friction on the finger covering material. In particular, it is probably important that the friction be neither too high (good sliding) nor too low (good grasping), and most importantly, exhibit no stiction, i.e. higher static than dynamic coefficient of friction. This will minimize fast transients as the finger breaks away from static conditions.

7 Conclusion

Compliance in robot hands has been shown to enhance grasping performance and robustness. This paper presents analysis and experiments to show that compliance also enables measurement of important object parameters using simple joint angle sensors. Compliance reduces control requirements so that it is easy to trace object surfaces, while joint angle measurements can reveal contact locations and contact force vectors. While these techniques are limited in the complexity of the contact situations where they can be applied, they are highly effective in many situations, and can be implemented at very low cost due to their use of existing joint angle sensors.

REFERENCES

- [1] Dollar, A. M. and Howe, R. D., 2010 "The Highly Adaptive SDM Hand: Design and Performance Evaluation," *International Journal of Robotics Research*, 29(5), pp. 585-597.
- [2] Dollar, A. M., Jentoft, L. P., Gao, J. D., and Howe, R. D., 2010, "Contact Sensing and Grasping Performance of Compliant Hands" *Autonomous Robots*, special issue on Mobile Manipulation, 28(1), pp. 65-75.
- [3] Tegin, J., and Wikander, J., 2005, "Tactile Sensing in Intelligent Robotic Manipulation a review ," *The Industrial Robot*, 32(1), pp. 64-70.
- [4] Jacobsen, S. C. , McCammon, I. D., Biggers, K. B., Phillips, R. P., 1988, "Design of Tactile Sensing Systems for Dexterous Manipulation," *IEEE Controls System Magazine*, 8(1), pp. 3-13.
- [5] Howe, R. D., and Cutkosky, M. R., 1992, "Touch sensing for robotic manipulation and recognition," in O. Khatib et al., (Ed.), *Robotics Review 2*, Cambridge: MIT Press, pp. 55-112.
- [6] Fearing, R. S., 1987, "Some Experiments with Tactile Sensing during Grasping," *Proc. of the 1987 Intl. Conf. on Robotics and Automation (ICRA 1987)*, pp. 1637-1643.
- [7] Lee, M. H., and Nicholls, H. R., 1999, "Tactile Sensing for Mechatronics: A State of the Art Survey," *Mechatronics*, 9(1), pp. 1-31 199
- [8] Dollar, A. M. and Howe, R. D., 2007, "Simple, Robust Autonomous Grasping in Unstructured Environments," *Proceedings of the 2007 International Conference on Robotics and Automation (ICRA 2007)*.
- [9] Merz, R., Prinz, F. B., Ramaswami, K., Terk, M., Weiss, L., 1994, "Shape Deposition Manufacturing," *Proc. 1994 Solid Freeform Fabrication Symposium*
- [10] Clark, J. E., Cham, J. G., Baily, S. A., Froehlich, E. M., Nahata, P. K., Full, R.J., and Cutkosky, M. R., 2001, "Biomimetic design and fabrication of a hexapedal running robot," *Proceedings of the 2001 International Conference on Robotics and Automation (ICRA 2001)*.
- [11] Butterfass, J., Grebenstein, M., Liu, H., and Hirzinger, G., 2001 "DLR-Hand II: next generation of a dextrous robot hand." *Proceedings of the 2001 IEEE international conference on robotics and automation (ICRA 2001)*. pp. 109114.
- [12] Dollar, A. M., and Howe, R. D., 2005, "Towards Grasping in Unstructured Environments: Grasper Compliance and Configuraton Optimization," *Advanced Robotics*, vol. 19(5), pp. 523-543.
- [13] Ramsden, E., 2006, *Hall-effect Sensors: Theory and Application*, Newness-Elsevier, Oxford, UK, Chap. 1
- [14] Kaneko, M. Tani, K., 1994, "Contact Point Detection for Grasping an Unknown Object Using Self-Posture Changeability," *IEEE Trans. Robots and Automation* 10(3), pp. 355-367.
- [15] Bicchi, A., Salisbury, J. K., and Brock, D. L., 1993, "Contact Sensing from Force Measurements," *International Journal of Robotics Research*, 12(3), pp. 249-262.
- [16] Hartmann, M. J., 2001, "Active Sensing Capabilities of the Rat Whisker System," *Autonomous Robots*, 11(3), pp. 249254.
- [17] Kaneko, M., Kanayama, N., and Tuji, T., 1998, "Active Antenna for Contact Sensing," *IEEE Trans. on Robotics and Automation*, 14(2), pp. 278-291.
- [18] Bicchi, A., Salisbury, J. K., and Dario, P., 1989, "Augmentation of Grasp Robustness Using Intrinsic Tactile Sensing," *In Proc. IEEE Conf. on Robotics and Automation*, Scottsdale, AZ, USA. pp. 302-307.